# Effects of JPEG Compression on the Accuracy of Photogrammetric Point Determination

Zhilin Li, Xiuxiao Yuan, and Kent W.K. Lam


## Abstract

*An empirical investigation into the effects of JPEG compression on the accuracy of photogrammetric point determination (PPD) is described. A pair of black-and-white aerial photographs of a city, taken at a scale of 1:8000, was selected and scanned at a resolution of 25 μm. Eighteen image points were measured with the ISDM module of an Intergraph digital photogrammetric workstation (DPW), and the bundle adjustment of a single model was performed using WuCAPS$_{SGPS}$ (Wuhan GPS-supported bundle block adjustment software). In processing various JPEG compressed images with Q-factors from 1 to 100, the accuracy of the 3D coordinates of the pass points was assessed and compared with that obtained from the original images (i.e., without compression). The empirical results show that, when the compression ratios are under 10, the compressed image is near-lossless. In other words, the visual quality of JPEG compressed images is still excellent and the accuracy of manual image mensuration is essentially not influenced. However, no indication can be found from the results that a compression of 10 is the critical value or the optimum compression level for PPD. Indeed, it is clear that the degradation of accuracy in PPD is almost linear.*


## Introduction

As we know, aerial photogrammetry has two central tasks, i.e., to accurately locate and to correctly recognize ground objects from airborne/spaceborne remotely sensed imagery, i.e., to extract the positioning and attribute information of the objects from images. The former is known as photogrammetric point determination (PPD).

Conventional PPD is performed in a least-squares adjustment with photo observations based on a certain number of ground control points. The photo observations are obtained by manual mensuration on hardcopy photographs by means of an accurate comparator. The advantage of the operation is the small volume of photo observations requiring storage. Its disadvantage is that it is manual, less efficient, and frequently erroneous. With the development of computer and image processing technology, photogrammetry has stepped into the softcopy photogrammetric era. In softcopy photogrammetry, expensive photogrammetric instruments are replaced by a digital photogrammetric workstation (DPW) and most operations are implemented automatically, such as interior orientation, image mensuration, DTM generation, etc. However, all operations in a DPW are based on digital images. Hardcopy photographs must be converted into digital images by a scanner. Doing so will create a huge volume of data. For example, a black-and-white digital aerial image scanned at a resolution of 20 μm contains approximately 10,000 by 10,000 pixels or 100 Mbytes of data. Sometimes more than six images are processed at the same time to measure image points automatically. As a result, reduction in image data volume is a matter of great significance in softcopy photogrammetry. Such a reduction in data volume can be achieved by image compression techniques.

A number of mature compression techniques have been developed. They can be broadly classified into two categories: lossless compression, e.g., the Lempel-Ziv and JBIG methods (Howard *et al.*, 1998), and lossy compression, e.g., JPEG, fractal, and wavelet compression (Jackson and Hannah, 1993). Lossless compression reduces the number of bits required to represent an image such that the reconstructed image is numerically identical to the original one on a pixel-by-pixel basis. This is of course ideal for photogrammetric applications. However, the compression ratio for such a method is generally 2 to 4 times for remotely sensed imagery (Wang *et al.*, 2000). The other type of method, lossy compression, on the other hand, allows the degradation of a reconstructed image in exchange for a higher degree of compression in data volume. These degradations may or may not be visually apparent. In this study, attention is paid to the loss of geometric quality due to compression.

In recent years, image compression has been an important topic in photogrammetry. Some researchers have concentrated their efforts on developing compression algorithms for airborne and spaceborne remotely sensed imagery (Lammi and Sarjakoski, 1992; Memon, 1994; Algarni, 1996; Xuan and Hu, 1999; Wang *et al.*, 2000; Zhang *et al.*, 2000). Others evaluate the effects of compression on the information extracted from the compressed digital aerial images (Mikhail *et al.*, 1984; Nunes *et al.*, 1992; Tada *et al.*, 1993; Jaakkola and Orava, 1994; Lammi and Sarjakoski, 1995; Robinson *et al.*, 1995; Novak and Shahin, 1996; Reeves *et al.*, 1997) and classification from the compressed satellite imageries (Paola and Schowengerdt, 1995; Correa *et al.*, 1998). In this study, particular attention has been paid to the effect of compression on the accuracy of image mensuration and PPD. A particular type of compression technique, JPEG, will be investigated. JPEG is selected because it has been

Dept. of Land Surveying and Geo-Informatics, Hong Kong Polytechnic University, Kowloon, Hong Kong (lszlli@polyu.edu.hk).

X. Yuan is also with the School of Information Engineering, Wuhan University, Wuhan 430079, P.R. China (yxxqxhyw@public.wh.hb.cn).

K.W.K. Lam is also with Brilliant Technology Development Limited, Hong Kong

Photogrammetric Engineering & Remote Sensing
Vol. 68, No. 8, August 2002, pp. 847–853.

0099-1112/02/6808–847$3.00/0

considered as an industry standard and has been implemented in most DPWs.

Indeed, in this study, our only concerns are the effects of JPEG compression on the accuracy of image mensuration and the changing of the 3D positions of the pass points in photogrammetric adjustment. From the literature, as far as the authors could determine, no similar work has been done, although some investigations into mensuration on digital images have been carried out. For example, subpixel positioning of targets has been a research subject for a considerable length of time (Mikhail, 1984; Trinder, 1989, Tichem and Cohen, 1994), and the accuracy of digital target location can reach 0.02 pixel or better in ideal circumstances (Trinder *et al.*, 1995).

The paper is organized as follows. The next section briefly describes the basic principles of JPEG image compression. This is followed by an outline of the design of the experiments. The experimental results are then reported. Finally, an analysis of these results is given.

## Principles of the JPEG Compression Technique

JPEG is an acronym for Joint Photographic Experts Group. JPEG compression, which is the international standard adopted by the ISO for compressing still continuous-tone photographic images, was established by the JPEG committee. A brief description of the key concepts in JEPG image compression is given in this section, in order to make the test results more understandable and more meaningful. More detailed information can be found in Wallace (1991) and Pennebaker and Mitchell (1993).

### General Principle

It can be observed that, in most areas of an image, the gray values of adjacent pixels are highly correlated. This means that a great deal of information about the gray value of a pixel can be obtained by inspecting its neighbors. Therefore, image pixels can be represented by a smaller number of gray values (represented by a smaller number of bits) rather than the full range of 256 levels (i.e., 8 bits) through the removal or reduction of this correlation between these pixels. To achieve the best representation with a minimum number of bits for the representation of an image, image compression is normally performed in three steps:

- *Transform*: This procedure uses a mathematical transformation, e.g., discrete cosine transform (*DCT*), to transform the original image to a different coordinate basis so as to reduce the dynamic range of the gray values and to eliminate the correlation among the original gray values. After a transformation, the original image is transformed to a new domain, such as the frequency domain, and the number of gray values is much smaller than originally/previously.
- *Quantization*: In this step the transformed gray values are mapped onto a smaller and finite number of output levels, in order to reduce the number of possible output symbols. The reduction of the number of output symbols leads to degradation in the reconstructed image quality. Thus, the quantization stage is a lossy process.
- *Encoding*: To further reduce the size of the image data, one replaces the stream of small integers with a more efficient alphabet of variable-length characters. Huffman coding is a commonly used method.

The JPEG standard contains four modes of operation: sequential encoding, progressive encoding, lossless encoding, and hierarchical encoding. The sequential and progressive encoding methods are DCT-based and lossy encoding techniques. The lossless mode is based on a predictive method. The hierarchical mode encodes the image at multiple spatial resolutions using either the DCT-based compression or the lossless mode. Although JPEG provides a number of possibilities for encoding, it also gives a basic compression scheme—-baseline sequential encoding—for straightforward use. JPEG compression in Intergraph is based on baseline sequential encoding to reduce the volume of the original images. Figure 1 describes the sequential steps of the baseline JPEG compression scheme.

The JPEG baseline system starts by dividing the original image into 8 by 8 blocks. Each block is independently transformed into the frequency domain using the DCT. Next, the resulting DCT coefficients are normalized by applying a user-defined normalization array that is fixed for all blocks. The normalized coefficients are then uniformly quantized by rounding to the nearest integer. The quantized coefficients are formatted into a 1D vector using the zigzag-ordering scheme. This zigzag-ordering rearranges the coefficients in approximately decreasing order. Many coefficients towards the end of the array are zero. From the above description, one can easily imagine that different normalization arrays will yield different compression ratios and image quality. The level of compression of an image can be modified by changing this array, e.g., scaling it by a constant. This multiplicative constant is generally called the quality factor (Q-factor). Finally, a lossless encoding module, Huffman encoding, is used to encode the quantitized coefficients. The resultant image is efficiently compressed and can be reproduced with virtually no visibly detectable loss.

### Image Compression Ratio

The image compression ratio is generally defined as the ratio of the number of bytes of the original image before compression to the number of bytes of the compressed image. It can be expressed as follows:

$$Ratio = \frac{original\ image\ data\ volume}{compressed\ image\ data\ volume}. \qquad (1)$$

For an $n$-bit image, the maximum compression ratio that can be achieved without any loss of information can be written as

$$Ratio_{max} = \frac{\log_2 M}{H} \qquad (2)$$

where $M = 2^n$ is the gray levels of the image and $H$ is the image entropy, expressing the minimum number of bits necessary for the representation of an image without any loss of information.

The maximum compression ratio can be achieved when the image coding, resulting in bits-per-pixel rates, is equal to the image entropy.

### Measures for Evaluating the Quality of a Compressed Image

In image compression, the quality of a reconstructed image can be evaluated by two measures: fidelity and peak signal-to-noise ratio (PSNR). Fidelity is the similarity between the original and the reconstructed image, i.e. it is a measure of the geometric distortion of the reconstructed image. However, PSNR represents radiometric degradation of the reconstructed image. For an 8-bit image with $m$ by $n$ pixels, it can be expressed as follows (Xuan and Hu, 1999):

$$Fidelity = \sum_{i=1}^{m}\sum_{j=1}^{n}(g_{ij} * g'_{ij}) / \sum_{i=1}^{m}\sum_{j=1}^{n} g_{ij}^2 \qquad (3)$$

$$PSNR = 20 \cdot \lg\left(\frac{255}{\delta}\right) = 48 - 20 \cdot \lg \delta \qquad (4)$$

where $g_{ij}$ and $g'_{ij}$ and are the gray values of the original and reconstructed images, respectively, and

$$\delta = \sqrt{\frac{1}{m \times n}\sum_{i=1}^{m}\sum_{j=1}^{n}(g_{ij} - g'_{ij})^2}$$

is the RMS that represents the gray differences between the original and reconstructed images. This is one numerical measure for determining the accuracy of a compressed image.

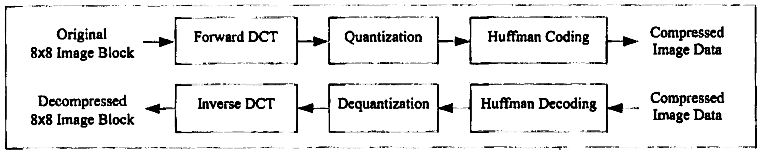


Figure 1. JPEG baseline compression scheme.

In lossless compression, the fidelity is 1.0 and the PSNR is infinite. When $\delta$ is equal to 1, the PSNR is 48.0 while, when $\delta$ equals 2, the PSNR is 42.0. One can regard image compression as near-lossless compression when the fidelity is more than 0.99 and the PSNR is above 42.0 (Xuan and Hu, 1999). Near-lossless compression means that the RMS of the gray values between pixels of the original and reconstructed images is less than the quantized noise in the radiometry, and positioning accuracy goes beyond the distortion of the sensor in the geometry.

## Design of this Experimental Study

### Platform and Test Area

JPEG has been implemented in all digital photogrammetric workstations (DPW). In this institution, an Intergraph DPW is available to the authors and was therefore used in this study.

A stereo pair of aerial photographs covering the Diamond Hill area of Hong Kong was used in this experiment (Figure 2). The photographs were taken from a flying height of about 1200 m (4,000 ft). The scale was 1:8,000. The area covers different land-cover types such as urban area with high rise buildings, a quarry site, a cemetery, and a hillside with medium vegetation coverage.

Approximately 160 Mbytes of raw image data were obtained by scanning these two photographs at a resolution of 25 $\mu$m using a Heleva scanner. Image mensuration was performed with the ISDM (ImageStation Digital Mensuration) tool of Intergraph DPW.

### Evaluation of the Effects of JPEG Compression on Image Quality

Equations 3 and 4, given in the previous section, address pictorial quality, i.e., how the pixel values are changed after compression, in comparison with the original image. This kind of measure is about visual satisfaction and is not of great interest to mapping scientists. Indeed, to this group of people, the geometric and thematic quality is the main concern.

Thematic quality means the accuracy of image classification. Classification accuracy is expected to decrease if compressed images are used. This is outside the scope of this study.

In this study, geometric quality is of great concern. Here geometric quality means the accuracy of photogrammetric measurement. Digital terrain models (DTM) and photogrammetric point determination (PPD) are typical results of photogrammetric measurement. An evaluation of the effect of JPEG compression on DTM accuracy has been conducted by Lam *et al.* (2001). In this paper, the effect of JPEG compression on the accuracy of PPD is investigated.

Because this investigation is about how JPEG compression affects PPD, only a relative evaluation was conducted. In other words, the 3D coordinates of the points determined using the original images were used as reference values. The 3D coordinates of the same points, determined using the images compressed at various levels, were then compared with the reference values to produce RMS values. The RMS values are used to indicate the quality of PPD. The distribution of the points to be evaluated is shown in Figure 3.

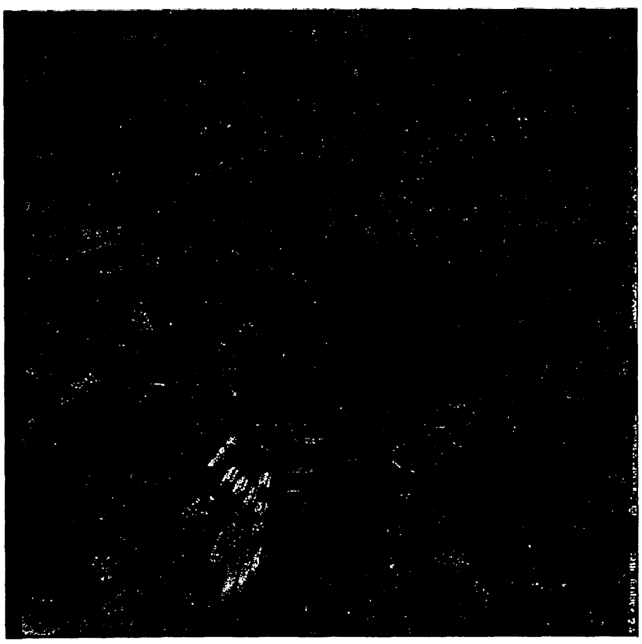

Figure 2. A photograph of the test area.

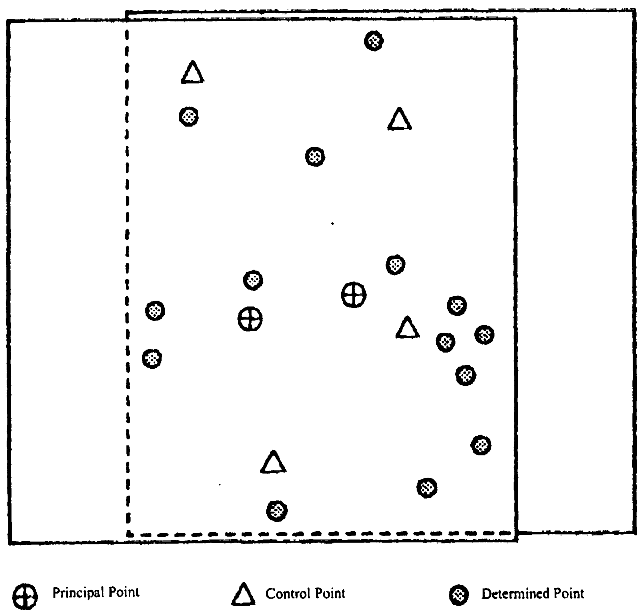


Figure 3. The distribution of photogrammetrically determined points.

Table 1. Accuracy of Interior Orientation in Left Image

| Q-Factor | 0 | 1 | 10 | 20 | 30 | 40 | 50 | 60 | 70 | 80 | 90 | 100 |
|---|---|---|---|---|---|---|---|---|---|---|---|---|
| Ratio | | 1.93 | 5.10 | 7.94 | 10.86 | 13.35 | 15.60 | 17.77 | 19.97 | 21.98 | 24.03 | 25.92 |
| Fidelity | | 1.000 | 1.000 | 1.000 | 1.000 | 1.000 | 0.998 | 0.998 | 0.998 | 0.998 | 0.998 | 0.998 |
| PSNR | | 54.55 | 43.16 | 41.25 | 40.23 | 39.41 | 38.76 | 38.20 | 37.69 | 37.23 | 36.81 | 36.45 |
| $\sigma_0/\mu m$ | 5.0 | 5.0 | 5.1 | 4.9 | 5.0 | 4.8 | 5.2 | 5.1 | 5.2 | 5.1 | 5.2 | 5.4 |

Table 2. Accuracy of Interior Orientation in Right Image

| Q-Factor | 0 | 1 | 10 | 20 | 30 | 40 | 50 | 60 | 70 | 80 | 90 | 100 |
|---|---|---|---|---|---|---|---|---|---|---|---|---|
| Ratio | | 1.92 | 5.08 | 7.84 | 10.77 | 13.25 | 15.46 | 17.56 | 19.68 | 21.62 | 23.60 | 25.42 |
| Fidelity | | 1.000 | 1.000 | 0.999 | 0.999 | 0.999 | 0.999 | 0.998 | 0.998 | 0.998 | 0.998 | 0.998 |
| PSNR | | 54.54 | 43.06 | 41.13 | 40.12 | 39.32 | 38.68 | 38.13 | 37.62 | 37.17 | 36.75 | 36.39 |
| $\sigma_0/\mu m$ | 4.9 | 4.9 | 5.1 | 5.0 | 5.1 | 5.3 | 5.0 | 5.5 | 5.5 | 5.6 | 5.2 | 5.5 |

#### Selection of Compression Level: Q-Factor vs Compression Ratio

As discussed above, in JPEG compression the compression level of an image can be controlled by a constant, which is generally called the quality factor (Q-factor). A higher Q-factor gives higher compression. A lower Q-factor gives a better quality image, but a lower compression ratio. Therefore, variable compression can be achieved by simply scaling the Q-factor. An important property of the JPEG scheme is the adjustment of the Q-factor to balance the reducing image size and degraded image quality. In fact, different JPEG compression programs have different Q-factors. In JPEG compression as applied in the Intergraph DPW, the Q-factors can be valued from 1 to 250 and the default value is 30.

In this experimental study, a number of compression levels with Q-factors ranging from 0 to 100 were tested, at intervals of 10. As a particular case, a compression level with Q-factor equal to 1 was also tested. In this particular case, the compression ratio varies from 1 (i.e., when Q = 0) to 26 (i.e., when Q = 100).

## Experimental Testing and Results

#### Procedures

In this study, the pair of digital images was first compressed at various levels, using Q = 0, 1, 10, 20, . . ., 100. The Ratio, Fidelity, and PSNR of the left and right images are listed in Tables 1 and 2, respectively. Figure 4 shows the effect of changing the Q-factors on compression ratio and PSNR.

PPD was implemented in each of these compression settings. Each of these compressed image pairs was used for PPD. PPD consists generally of three steps:

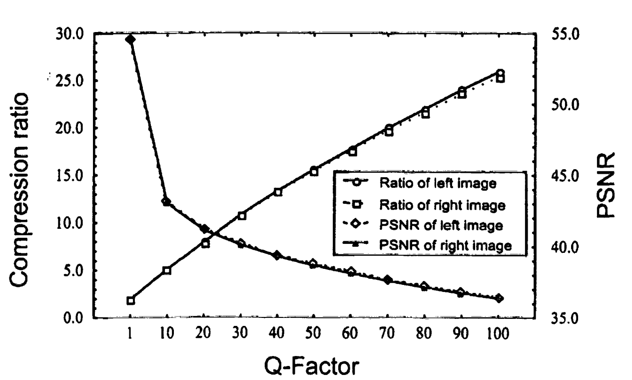


Figure 4. Compression ratio and PSNR vs. Q-factors.

- image mensuration,
- field survey of ground control points, and
- photogrammetric adjustment of image observations based on the minimum number of ground control points.

The flow chart of photogrammtric point determination is as shown in Figure 5.

#### Effect of JPEG Compression on the Accuracy of Orientations

The accuracy of the 3D coordinates of the photogrammetric points is influenced by the errors occurring in each of the three steps described above.

The interior orientation of the image is the first step in PPD, to establish the relationship between the pixel and the image coordinate system. It is always implemented through manual or automated mensuration of fiducial marks. The accuracy of the interior orientation is determined by using the RMS of the residuals of the 2D coordinates of the fiducial marks used. In this study, semi-automated interior orientation was performed using four fiducial marks in the image corners which were manually determined, and the accuracy of the interior orientation was 5.0 $\mu$m. This result is similar to those reported by others, e.g., 0.13 pixels by Lue (1997). The effect of JPEG compression on the accuracy of interior orientations is also shown in Tables 1 and 2.

The next step of PPD is relative orientation to determine the relative position and attitude of two images with respect to one another. After this step, a stereo model was formed by eliminating the $y$-parallax at all pass and tie points. The accuracy of relative orientation is determined by the RMS of all $y$-parallax residuals. Although automated relative orientation is fast, accurate, robust, and reliable (Heipke, 1997), the operators still had to manually measure all pass points in this study because only an Intergraph DPW without ISAT (ImageStation Match-AT, automated point measurement, and bundle adjustment program) was available to the authors and used in our test.

Eighteen passpoints well distributed over the model were then measured stereoscopically (Figure 3). These passpoints included four artificial points in the playgrounds, four corner points of some building tops, four control points pre-marked on buildings, and six identifiable object points. These points were very clear in both of the original images. A sample of these points is shown in Figure 6. In this figure, the effect of JPEG compression on the position determination of these passpoints is also shown. The effect of JPEG compression on the accuracy of relative orientation is shown in Figure 7.

In order to get the approximation of the exterior orientation elements and 3D coordinates of the passpoints, the stereo model was registered to the ground by absolute orientation. It was implemented by using three or more ground control points well distributed over the model. The RMS of the residuals of the

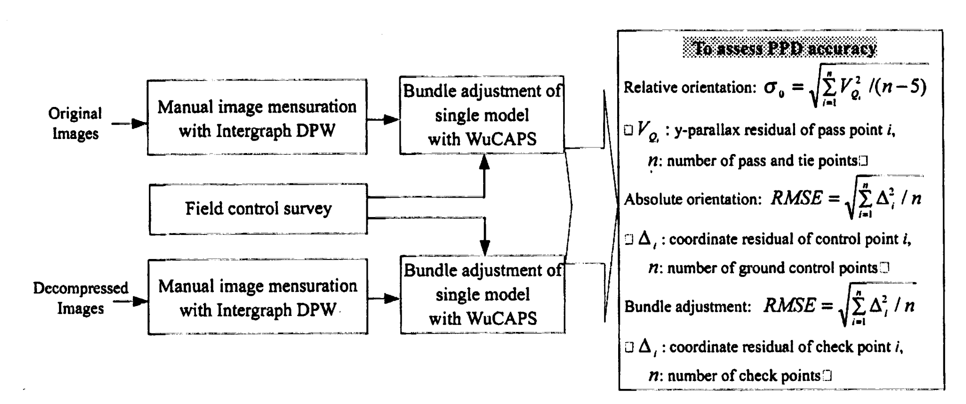


Figure 5. Flowchart of photogrammtric point determiniation.

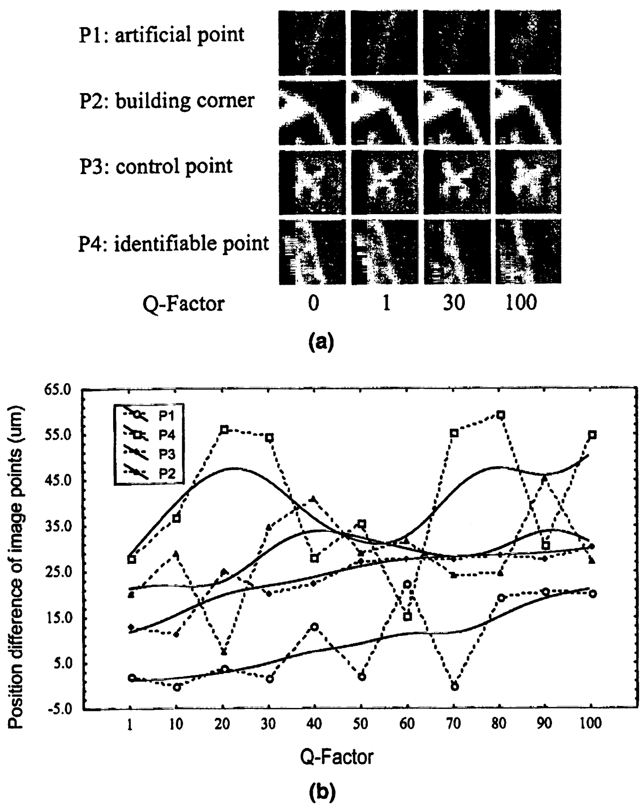


Figure 6. Position difference between original and JPEG compressed images vs. Q-factors. (a) Feature points at various Q-factors. (b) Position changes of points with Q-factors.

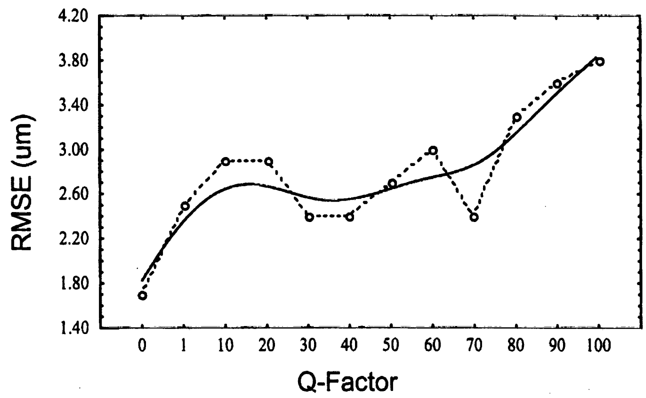


Figure 7. Accuracy of relative orientation vs. Q-factors.

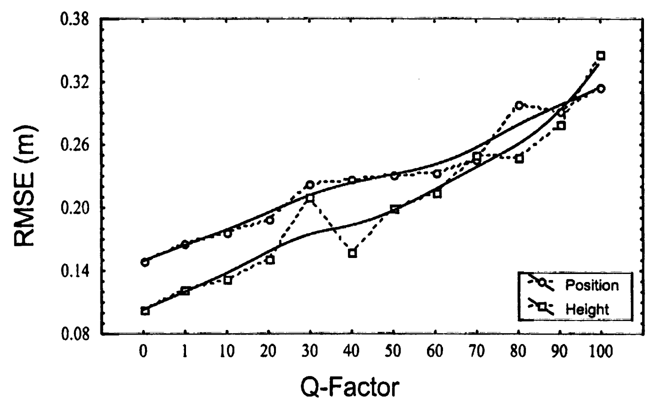


Figure 8. Accuracy of absolute orientation vs. Q-factors.

3D coordinates on these control points is used as a measure of the accuracy of absolute orientation. The effect of JPEG compression on the accuracy of absolute orientation is shown in Figure 8.

**Effect of JPEG Compression on the Accuracy of PPD**

The final step of PPD is the adjustment of image observations. In this study, bundle adjustment of a single model was carried out using $\text{WuCAPS}_{GPS}$, a GPS-supported bundle block adjustment system developed by Yuan (2000). The PPD result shows that the unit weight standard deviation of image measurements was $\sigma_0 = 2.8\ \mu\text{m}$, and the theoretical accuracy of the 3D coordinates of the pass points were $m_X = 4.7\ cm$, $m_Y = 5.2\ cm$, $m_{XY} = 7.0\ cm$, and $m_Z = 20.1\ cm$ on the ground, respectively.

The final PPD accuracy is interesting in photogrammetric applications and is often assessed by using the RMS of the 3D coordinates of all checkpoints. In this study, 14 passpoints, excluding control points, were used as checkpoints. As stated

TABLE 3. ACCURACY OF PPD WITH JPEG COMPRESSED IMAGE PAIRS

| Q-Factor | Relative orientation $\sigma_0$ ($\mu$m) | Absolute orientation (m) | | | | Bundle adjustment (m) | | | | | Accuracy degeneration (%) | |
|---|---|---|---|---|---|---|---|---|---|---|---|---|
| | | $X$ | $Y$ | $XY$ | $Z$ | $\sigma_0$ ($\mu$m) | $X$ | $Y$ | $XY$ | $Z$ | $XY$ | $Z$ |
| 0 | 1.7 | 0.05 | 0.14 | 0.149 | 0.103 | 2.8 | 0.047 | 0.052 | 0.070 | 0.201 | | |
| 1 | 2.5 | 0.08 | 0.15 | 0.167 | 0.122 | 5.4 | 0.13 | 0.22 | 0.254 | 0.270 | 262 | 34 |
| 10 | 2.9 | 0.08 | 0.16 | 0.176 | 0.133 | 7.3 | 0.07 | 0.26 | 0.272 | 0.334 | 288 | 66 |
| 20 | 2.9 | 0.11 | 0.15 | 0.190 | 0.151 | 5.7 | 0.17 | 0.20 | 0.268 | 0.341 | 283 | 70 |
| 30 | 2.4 | 0.10 | 0.20 | 0.222 | 0.210 | 6.5 | 0.15 | 0.24 | 0.288 | 0.346 | 311 | 72 |
| 40 | 2.4 | 0.12 | 0.19 | 0.226 | 0.157 | 5.6 | 0.13 | 0.29 | 0.312 | 0.395 | 346 | 96 |
| 50 | 2.7 | 0.12 | 0.20 | 0.232 | 0.200 | 5.9 | 0.17 | 0.28 | 0.329 | 0.417 | 370 | 107 |
| 60 | 3.0 | 0.12 | 0.20 | 0.234 | 0.215 | 8.2 | 0.18 | 0.28 | 0.332 | 0.406 | 374 | 102 |
| 70 | 2.4 | 0.11 | 0.22 | 0.245 | 0.251 | 4.6 | 0.16 | 0.33 | 0.367 | 0.409 | 424 | 103 |
| 80 | 3.3 | 0.14 | 0.24 | 0.298 | 0.247 | 8.2 | 0.16 | 0.30 | 0.341 | 0.452 | 387 | 125 |
| 90 | 3.6 | 0.15 | 0.25 | 0.291 | 0.280 | 7.0 | 0.21 | 0.33 | 0.391 | 0.491 | 458 | 144 |
| 100 | 3.8 | 0.15 | 0.28 | 0.316 | 0.347 | 7.0 | 0.20 | 0.36 | 0.412 | 0.555 | 488 | 176 |

Remarks:
(1) Q-Factor = 0 denotes original image. The accuracy of the bundle adjustment is theoretical accuracy $m_i = \sigma_0 \sqrt{(\mathbf{Q}_{XX})_i}$, ($i = X, Y, XY, Z$), where $\sigma_0$ is the unit weight standard deviation of image measurements; $\mathbf{Q}_{XX}$ is the variance-covariance matrix.
(2) Q-Factor from 1 to 100 denotes JPEG compressed images with various levels. The accuracy of the bundle adjustment is the root-mean-square errors of coordinate differences of passpoints, i.e., $\mu_i = \sqrt{\Sigma\Delta_i^2/14}$ ($i = X, Y, Z$); $\mu_{XY} = \sqrt{\mu_X^2 + \mu_Y^2}$.
(3) The accuracy degeneration of PPD is $(\mu_i - m_i)/m_i$, ($i = XY, Z$).

previously, the 3D coordinates of these points, determined using the original image pair, were used as reference values and, therefore, the accuracy assessment is used to compare other 3D coordinates of the checkpoints with these reference values. The comparison was done on a point-by-point basis (see Table 3). The results are shown in Table 3 and Figure 9. As stated previously, this accuracy is shown in a relative sense.

## Analysis of Results

Figure 4 shows that the compression ratios increase almost linearly and image quality falls with an increase in the Q-factor. It can also be seen that there is a sudden transition in image quality on compressing with Q-factors of 1 to 10. The degradation trends of the image quality were then slow with increasing compression ratios. According to the criteria in the section on Principles of the JPEG Compression Technique, the compressions are near-lossless when Q-factors are under 20. When Q-factors are over 20, the compressions are lossy. From this experiment, it can be noted that the JPEG compression with a Q-factor of 30 (or compression ratio equal to 10), which is recommended by Intergraph DPW, is near-lossless.

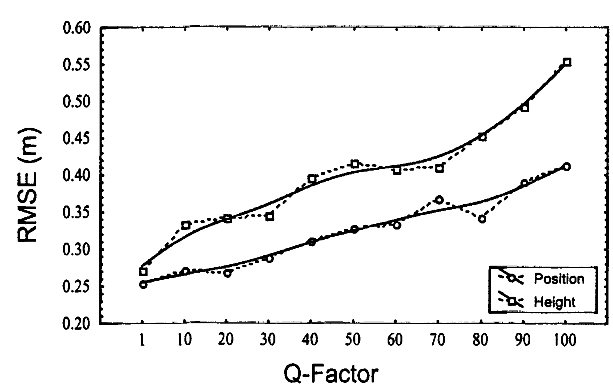


Figure 9. Overall (relative) accuracy of bundle adjustment vs. Q-factors.

From Tables 1 and 2, it can be concluded that the accuracy of interior orientation remains almost unchanged with an increase in Q-factor (up to 100). This is because, although the images of fiducial marks become more blurred with the increase in compression ratios, one can still recognize and accurately locate their central points due to their very regular "cross" shapes. In addition, some systematic errors, for example, geometric distortion, are compensated by the affine transform in the adjustment of interior orientation. In this study, it is found that the geometric distortion of the compressed images is small, and the image coordinate system is not affected when the compression ratio is under 25. This is very important in softcopy photogrammetry.

Figure 7 shows that the higher the compression ratio, the poorer the accuracy of the relative orientation. The increase in RMS is almost linear when the Q-factor is smaller than 10 and larger than 70. From Q = 0 to Q = 100, the RMS value increased twofold. This is a consequence of the change in the positions of the feature points used for relative orientation. As shown in Figure 6, such a change in position for artificial points, building corners, and control points is very clear.

Figure 8 shows the variation of the RMS of absolute orientation with compression ratio. With an increase in compression ratio, the increase in RMS is quite linear, and the RMS in position is larger than that in height.

Figure 9 depicts the RMS of PPD in both position and height. These RMS values are computed from the differences on all checkpoints both in planimetry and height. From this figure, it can be seen that PPD accuracy falls off rapidly with an increase in compression ratio. It seems that the increase is also quite linear. Table 3 lists the detailed quantification of the RMS degeneration:

- 263 percent in planimetry and 34 percent in height for a Q-factor of 1,
- 311 percent in planimetry and 72 percent in height for a Q-factor of 30, and
- 488 percent in planimetry and 176 percent in height for a Q-factor of 100.

On the other hand, if one only looks at the results from Q = 1, then the increase in RMS is not that great. From Figure 9 it also appears that the RMS values in height for Q = 10, 20, and 30 are almost identical. This might be the reason that the Intergraph recommends a compression ratio of 10:1, which corresponds to a Q-factor of 25 in this case.

## Conclusions

In this paper, an experimental investigation into the effect of JPEG compression on the accuracy of PPD is reported. The experiment was conduced on an Intergraph DPW. A review of JPEG compression on the Intergraph DPW is first given; the design of this study is then outlined, followed by a report of the results. An analysis of the results is also presented. Instead of discussing only the final results of PPD, the intermediate results for interior, relative, and absolute orientations are also reported and analyzed. It is hoped that this will provide a more complete picture.

The empirical results show that, when the compression ratios are smaller than 10, the JPEG compression is near-lossless. This means that the visual quality of the compressed images is still excellent, i.e., without noticeable degeneration in pictorial quality. Theoretically speaking, in such a case, manual mensuration is still of great accuracy, and the accuracy loss in the final PPD is acceptable for most photogrammetric applications. However, no indication can be found from the results that a compression of 10 is the critical value or the optimum compression level for PPD. Indeed, it is clear that the degradation of accuracy in PPD is almost linear.

## Acknowledgments

The work described in this paper was supported by a grant from the Research Grants Council of the Hong Kong Special Administrative Region (Project No. PolyU 5091/97E). The authors would also like to express their thanks to Professor Jiabin Xuan and Mr. Qingwu Hu of the Wuhan Technical University of Surveying and Mapping for providing their compression software for testing.

## References

Algarni, D.A., 1996. Compression of remotely sensed data using JPEG, *International Archives of Photogrammetry and Remote Sensing*, 31(B3):24–28.

Correa, A.C., A.J. Blanchard, and J. Becker, 1998. The impact of lossy compression on the output of supervised and unsupervised classification products, *Proceedings of International Geoscience and Remote Sensing Symposium*, 06–10 July, Seattle, Washington, 4:1745–1747.

Heipke, C., 1997. Automation of interior, relative, and absolute orientation, *ISPRS Journal of Photogrammetry & Remote Sensing*, 52(1):1–19.

Howard, P.G., F. Kossentini, B. Martins, S. Forchhammer, and W.J. Rucklidge, 1998. The emerging JBIG2 standard, *IEEE Transactions on Circuits and Systems for Video Technology*, 8(7):838–848.

Jaakkola, J., and E. Orava, 1994. The effect of pixel size and compression on metric quality of digital aerial images, *International Archives of Photogrammetry and Remote Sensing*, 30(3/1):409–415.

Jackson, D.J., and S.J. Hannah, 1993. Comparative analysis of image compression techniques, *Proceedings SSST '93, The 25th Southeastern Symposium on System Theory*, March, Tuscaloosa, Alabama, pp. 513–517.

Lam, K., Z.L. Li and X.X. Yuan, 2001. Effect of JPEG compression on the Accuracy of DTM, *Photogrammetric Record*, 17(98):331–342.

Lammi, J., and T. Sarjakoski, 1992. Compression of digital color images by the JPEG, *International Archives of Photogrammetry and Remote Sensing*, 29(B2):456–460.

———, 1995. Image compression by the JPEG algorithm, *Photogrammetric Engineering & Remote Sensing*, 61(10):1261–1266.

Lue, Y., 1997. One step to a higher level of automation for softcopy photogrammetry automated interior orientation, *ISPRS Journal of Photogrammetry & Remote Sensing*, 52(3):103–109.

Memon, N.D., K. Sayood, and S.S. Magliveras, 1994. Lossless compression of multispectral image data, *IEEE Transactions on Geoscience and Remote Sensing*, 32(2):282–289.

Mikhail, E.M., M.L. Akey, and O.R. Mitchell, 1984. Detection and subpixel location of photogrammetric targets in digital images, *Photogrammetria*, 39(3):63–83.

Nunes, P.R.R.L., A. Alciam, and M.R.L.F. da Silva, 1992. Compression of satellite images for remote sensing applications, *International Archives of Photogrammetry and Remote Sensing*, 29(B2): 479–483.

Novak, K., and F.S. Shahin, 1996. A comparison of two image compression techniques for softcopy photogrammetry, *Photogrammetric Engineering & Remote Sensing*, 62(6):695–701.

Paola, J.D., and R.A. Schowengerdt, 1995. The effect of lossy image compression on image classification, *Proceedings of International Geoscience and Remote Sensing Symposium—Quantitative Remote Sensing for Science and Applications*, 10–14 July, Florence, Italy, 1:118–120.

Pennebaker, W.B., and J.L. Mitchell, 1993. *JPEG Still Image Data Compression Standard*, Van Nostrand Reinhold, New York, N.Y., 638 p.

Reeves, R., K. Kubik, and Y.H. Lu, 1997. JPEG comparison and DTM accuracy, *Technical Papers of 1997 ACSM/ASPRS Annual Convention and Exposition*, 07–10 April, Seattle, Washington, 2:342–346.

Tada, T., K. Cho, H. Shimoda, and T. Sakata, 1993. An evaluation of JPEG compression for on-line satellite image transmission, *Proceedings IGARSS'93, Geoscience and Remote Sensing Symposium on Better Understanding of Earth Environment*, 18–21 August, Tokyo, Japan, 3:1515–1518.

Tichem, M., and M.S. Cohen, 1994. Sub$\mu$m registration of fiducial marks using machine vision, *IEEE Transactions on Pattern Analysis and Machine Intelligence*, 16(8):791–794.

Trinder, J.C., 1989. Precision of digital target location, *Photogrammetric Engineering & Remote Sensing*, 55(6):883–886.

Trinder, J.C., J. Jansa, and Y. Huang, 1995. An assessment of the precision and accuracy of methods of digital target location, *ISPRS Journal of Photogrammetry & Remote Sensing*, 50(2):12–20.

Wallace, G.K., 1991. The JPEG still picture compression standard, *Communication of ACM*, 34(4):27–142.

Wang, C.S., B.X. Yu, Y.S. Dai, and D.H. Wen, 2000. A transform coding compression of hyperspectral image with its edge features retained, *Journal of Remote Sensing*, 4(2):95–99 (in Chinese).

Xuan, J.B., and Q.W. Hu, 1999. The technique of quasi-lossless compression of remote sensing image, *Journal of Wuhan Technical University of Surveying and Mapping*, 24(4):290–294 (in Chinese).

Yuan, X.X., 2000. Principle, software and experiment of GPS-supported aerotriangulation, *Geo-Spatial Information Science*, 3(1):24–33.

Zhang, R., Z.K. Liu, and S. Zhan, 2000. Wavelet-based compression for multispectral imagery, *Journal of Remote Sensing*, 4(2):100–105 (in Chinese).

(Received 03 January 2001; accepted 16 January 2002; revised 07 February 2002)